GNSS L5/E5a Code Properties in the Presence of a Blanker

Seunghwan Kim, Nicolas Gault, Yongrae Jo, Hyosang Yoon, Byungwoon Park, Axel Garcia-Pena, Christophe Macabiau, Dennis Akos

Received: 27 August 2024 | Revised: 7 February 2025 | Accepted: 5 May 2025

DOI: 10.33012/navi.700

ORIGINAL ARTICLE

GNSS L5/E5a Code Properties in the Presence of a Blanker

Seunghwan Kim[1] | **Nicolas Gault**[2] | **Yongrae Jo**[3] | **Hyosang Yoon**[1] | **Byungwoon Park**[3] | **Axel Garcia-Pena**[2] | **Christophe Macabiau**[2] | **Dennis M. Akos**[4]

[1] Korea Advanced Institute of Science and Technology (KAIST)

[2] École Nationale de l'Aviation Civile (ENAC)

[3] Sejong University

[4] University of Colorado Boulder

Correspondence
Seunghwan Kim
N7-2, 291, Daehak-ro, Yuseong-gu, Daejeon, Republic of Korea
Email: shkimkaist@kaist.ac.kr

Abstract

Modern global navigation satellite system L5/E5a code families offer improved correlation properties, with lower auto-correlation sidelobes and cross-correlations, compared with legacy Global Positioning System L1 coarse/acquisition (C/A) codes. However, these codes encounter unique L5/E5a interference environments, particularly those including interference due to pulses from distance-measuring equipment and tactical air navigation systems. In civil aviation, temporal blanking is the assumed countermeasure. In temporal blanking, incoming samples are set to zero when the peak envelope power exceeds a threshold, blanking the codes within the sampled signals and affecting their correlation with non-blanked replicas. Through extensive simulations, this study analyzes L5/E5a code properties under blanking duty cycle (*bdc*) values of 0%–75% over a 1-ms integration time. Results indicate reduced auto-correlation and cross-correlation protections, although these effects remain superior to those of L1 C/A codes until *bdc* reaches approximately 60%. Further increases in *bdc* to 75%, likely due to increasing air traffic, diminish these advantages. Additionally, simulations show that Doppler residuals have a minimal impact on L5/E5a correlation properties.

Keywords

blanker, code properties, Doppler residuals, GNSS, L5 band

1 | INTRODUCTION

In 1999, the United States announced its intention to radiate a new Global Positioning System (GPS) signal in the L5 band centered at 1176.45 MHz, GPS L5, with advanced design features such as the introduction of a data component GPS L5I and a dataless (pilot) component GPS L5Q (IS-GPS-705J, 2022). In the same year, the European Space Agency initiated the definition phase of a new navigation satellite system called Galileo, which provides navigation signals on three frequencies, including the E5 band centered at 1191.795 MHz (European Space Agency, 1999). Specifically, the E5a signal is also centered in the L5 band and comprises the data/pilot pair E5a-I/Q (Falcone et al., 2017). Both GPS L5 and Galileo E5a are direct-sequence spread-spectrum signals using code division multiple access (CDMA). CDMA allows the receiver to identify the satellite sending a signal and to determine the code delay and Doppler frequency of the received

global navigation satellite system (GNSS) signals by means of a correlation operation (Kaplan & Hegarty, 2005). For both the GPS L5 and Galileo E5a signals, the families of codes used to achieve this goal were carefully chosen to have excellent correlation properties, thereby minimizing the probability of missed or false detections.

Since then, some properties of the GPS L5I/Q and Galileo E5a-I/Q codes have been analyzed. For GPS L5 codes, the maximum auto-correlation secondary peak was found to be −29.2 dB for L5I and −29.0 dB for L5Q, with the cross-correlation peak at −26.4 dB for L5I and −26.5 dB for L5Q (Macabiau et al., 2002; Tran, 2004). For Galileo E5a, the maximum auto-correlation secondary peak was −28.9 dB for E5a-I and −28.7 dB for E5a-Q, and the cross-correlation peak was −26.0 dB for E5a-I and −25.5 dB for E5a-Q (Miret, 2005; Gao, 2008). Thus, both the GPS L5 and Galileo E5a signals provide better auto- and cross-correlation protection than the legacy GPS L1 coarse/acquisition (C/A) pseudorandom noise (PRN) codes, which have a maximum auto-correlation secondary peak and cross-correlation peak of approximately −24 dB (Morton et al., 2003; Foucras et al., 2017). Betz et al. (2006) provided a broader summary of the correlation properties of several GNSS code families, including L5 and E5a, with a code length of 10,230 chips.

In addition to improved correlation protection, the L5/E5a signals also provide improved multipath performance, protection against narrowband interference, and ionospheric delay correction when combined with signal measurements from other bands. For these reasons, GPS L5 and Galileo E5a signals are of special interest for civil aviation, and the next generation of airborne GNSS receivers, with dual-frequency multi-constellation (DFMC) capabilities, will be able to process both signals (Tran, 2004; Novella et al., 2022).

However, the GNSS L5/E5a radio frequency interference (RFI) environment is dominated by existing pulsed systems such as distance-measuring equipment (DME), tactical air navigation (TACAN) systems, the Joint Tactical Information Distribution System (JTIDS), and the Multifunctional Information Distribution System (MIDS), which co-exist in the L5/E5 GNSS frequency band and impact the nominal processing of GNSS receivers. In the context of civil aviation, a long thread of activities has led to an elaboration of various standards by the International Civil Aviation Organization, the Radio Technical Commission for Aeronautics (RTCA), and the European Organization for Civil Aviation Equipment to determine and bound the vulnerability of DFMC GNSS receivers to these RFI sources in the L5/E5a band. In the standards, a temporal blanker is assumed to be implemented in the radio frequency front-end (RFFE) block of the GNSS DFMC receiver to mitigate the impact of the pulsed RFI observed in the L5/E5a band (RTCA, 2004). The role of the blanker is to set the incoming signal samples to zero whenever the peak envelope power of a received pulse exceeds a fixed threshold (Hegarty et al., 2000; Grabowski & Hegarty, 2002; Garcia-Pena et al., 2019; Garcia-Pena, Macabiau, Julien et al., 2020; Garcia-Pena, Macabiau, Novella et al., 2020). Depending on the RFI scenario (e.g., number of beacons, received power at the aircraft level, pulse time of arrival, etc.), the blanking duty cycle (*bdc)*, i.e., the percentage of samples set to zero by the blanker, is determined. A worst-case scenario was found in RTCA DO-292 at Harrisburg, PA, at a high altitude (flight level [FL] 400), where *bdc* reached up to 63%, owing to a high number of DME/TACAN beacons (RTCA, 2004).

In the blanking process, parts of the useful incoming GNSS signal are also blanked as well as the incoming L5I/Q and E5a-I/Q codes, which are later correlated with unblanked code replicas in the acquisition and tracking stages. Therefore, the results found in the literature concerning the GPS L5I/Q and Galileo E5a-I/Q code properties are no longer applicable in the presence of a

blanker. Furthermore, in practice, GNSS signals are always received with additional Doppler residuals caused by satellite and receiver motion, which cause a frequency offset between the incoming signal and the local replica (Van Diggelen, 2009). Therefore, the auto- and cross-correlation properties must be investigated in the presence of Doppler residuals.

In the literature, the auto- and cross-correlation properties have been thoroughly assessed for the GPS L1 C/A Gold codes (Gold, 1967) and Galileo E1 signals. These properties have been addressed in previous studies, particularly in the presence of Doppler offsets (Spilker, 1996; Soualle et al., 2005; Wallner et al., 2007; Soualle, 2009; Qaisar & Dempster, 2011). Foucras et al. (2017) expanded this discussion by providing comprehensive statistics on the auto- and cross-correlation properties with Doppler residuals ranging from –10 to 10 kHz for all pairs of GPS L1 and Galileo E1 codes.

However, for the L5/E5a band, to the authors' best knowledge, the only works that consider Doppler residuals are those of Spilker and Van Dierendonck (2001) for L5 and Gao and Enge (2012) for E5a. The former study examined the impact of Doppler shifts on L5 codes, but the analysis was limited to a few selected L5 codes, with correlation properties assessed at a Doppler step of 1 kHz. Gao and Enge (2012) provided correlation properties in the presence of Doppler residuals ranging from –10 to 10 kHz, but this work was limited to the first two test satellites of the Galileo E5a system, Galileo In-Orbit Validation Elements, which are no longer active. Therefore, the literature still lacks an exhaustive study on the auto- and cross-correlation properties of the L5/E5a code in the presence of Doppler residuals and, more importantly, in the presence of blanking for future DFMC civil aviation receivers. In this work, statistics on the auto-correlation main peak, auto-correlation secondary peak, and cross-correlation peak (including maximum values and quantiles) are provided, with a primary focus on the impact of blanking, with *bdc* ranging from 0% to 75% (covering the RTCA DO-292 worst-case scenario). This paper also examines the L5/E5a code properties in the presence of Doppler residuals ranging from –10 to 10 kHz in the no-blanking case.

This paper is organized as follows. Section 2 presents the motivation for this work and explains its focus. Section 3 provides an overview of the GPS L5/Galileo E5a signal structures and describes a generic airborne GNSS DFMC receiver. Section 4 introduces the simulation methodology used to obtain statistics on the GPS L5 and Galileo E5a code properties in the presence of Doppler residuals or blanking. Section 5 presents and discusses simulation results for the auto-correlation and cross-correlation of GPS L5 and Galileo E5a. Finally, the study is concluded in Section 6.

2 | MOTIVATION AND DOPPLER RESIDUAL

This study is motivated by the omnipresence of DME/TACAN RFI signals in the GNSS L5/E5a band. Indeed, the number of received RFI pulses at airborne GNSS DFMC receivers may be very high, as each DME/TACAN ground beacon in the aircraft radio line of sight can simultaneously respond to the interrogations of multiple aircraft, potentially triggering the blanker multiple times. Therefore, the GNSS L5/E5a code properties must be investigated in blanking conditions, that is, by correlating a blanked and an unblanked version of the code replica. The number of blanked samples is determined by the worst-case scenario initially defined in the standards (2004), where up to 63% of the received signal is assumed to be

blanked at Harrisburg, PA, i.e., *bdc* = 0.63 (RTCA, 2004). However, air traffic volume grows every year and is expected to exceed the pre-COVID-19 pandemic level by 2025 (Airbus, 2024), indicating that higher *bdc* values may be found in in the near future. Moreover, two recent experimental studies have shown in-phase/quadrature (I/Q) sample recordings exhibiting high blanking levels due to the presence of strong DME/TACAN multipath signals (Zeta Associates, 2019, 2021), which are currently not considered in the RTCA DO-292 worst-case derivation. For these reasons, the GNSS L5/E5a code properties are investigated in this study for *bdc* values not simply ranging from 0% to 63% but from 0% to 75%, to anticipate the worst values of *bdc*.

GNSS code properties are classically evaluated in the presence of Doppler residuals. This is the case for the properties of GNSS L1/E1 code, as indicated in Section 1 (Spilker, 1996; Soualle et al., 2005; Wallner et al., 2007; Soualle, 2009; Qaisar & Dempster, 2011; Foucras et al., 2017). However, simulation results have shown that the effect of Doppler residuals is negligible when considering the GNSS L5/E5a code families (simulation results shown in Section 5). Therefore, this study primarily focuses on the blanking effect only.

3 | SIGNAL DEFINITION AND GENERIC AIRBORNE GNSS DFMC RECEIVER SCHEME

3.1 | GPS L5 and Galileo E5a Signal Definition

The GPS L5 signal transmitted by satellite i is a quadrature phase shift keying (QPSK) modulation applied to the L5 carrier, consisting of both data and pilot channels. The mathematical model of this signal is as follows:

$$s^i_{L5}(t) = Ad^i(t)\, c^s_{L5I}(t)\, c^{p,i}_{L5I}(t) \cos\left(2\pi f_{L5} t\right) + Ac^s_{L5Q}(t)\, c^{p,i}_{L5Q}(t) \sin\left(2\pi f_{L5} t\right) \quad (1)$$

In this equation, A is the signal amplitude, where the minimum total power of the received GPS L5 signal is either −157 dBW (block III/IIIF) or −157.9 dBW (block IIF) for both the data and pilot channels (IS-GPS-705J, 2022). The term d^i represents the L5 navigation message encoded by a convolutional forward error correction (FEC) encoder with a ½ rate for satellite *i*. The original L5 navigation message has a data rate of 50 bps, whereas d^i has a final rate of 100 sps after encoding, resulting in a symbol duration of 10 ms. The sequences c^s_{L5I} and c^s_{L5Q} are the 10-bit and 20-bit secondary Neuman–Hofman codes (Neuman & Hofman, 1971), respectively, encoded in the polar non-return-to-zero level (P/NRZ/L) form. These codes are clocked at a rate of 1 kHz, giving each bit a duration of 1 ms. Meanwhile, $c^{p,i}_{L5I}$ and $c^{p,i}_{L5Q}$ represent the primary data and pilot component PRN codes specific to satellite *i*, respectively. The codes, also in the P/NRZ/L form, are 10,230 chips long and are clocked at a rate of 10.23 MHz, resulting in a code period of 1 ms. Finally, the carrier frequency for the L5 band, denoted as f_{L5}, is 1176.45 MHz.

The c^p_{L5I} and c^p_{L5Q} PRN codes are generated as the modulo-2 sum of two different sequences generated by two linear feedback shift registers (LFSRs). Detailed information on the GPS L5 code generation process can be found in IS-GPS-705J (2022). The correlation properties of 37 GPS L5 codes retrieved from Macabiau et al. (2002) and Tran (2004), which do not consider Doppler residuals or blanking, are summarized in Table 1.

The Galileo E5a signal is transmitted as part of the multiplexing of Galileo E5a and E5b signals, constituting the wideband Galileo E5 signal. Each E5a and E5b

TABLE 1
c^p_{L5I} and c^p_{L5Q} Code Properties Without Considering Doppler Residuals or Blanker

Max. Auto-Correlation Sidelobe (dB)		Max. Cross-Correlation (dB)	
c^p_{L5I}	c^p_{L5Q}	c^p_{L5I}	c^p_{L5Q}
−29.2	−29.0	−26.4	−26.5

signal consists of two components, the data component and the pilot component. The four components are transmitted at the same time, while being separated in frequency owing to an alternative binary offset carrier (Alt-BOC) modulation (OS SIS ICD, 2023; Rebeyrol, 2007).

Because of the widely split spectrum generated by the Alt-BOC modulation, it is possible to receive the E5a (or E5b) signal as a pure QPSK(10) signal as long as the front-end filter of the receiver has a bandwidth of less than 51.15 MHz (Tawk et al., 2012). As future airborne DFMC receivers are expected to operate with a front-filter frequency of 12–20 MHz (RTCA 2004), only the pure QPSK(10) is considered for this analysis. Under this assumption, the Galileo E5a signal radiated by satellite i is modeled as follows:

$$s^i_{E5a}(t) = Ad^i(t)c^{s,i}_{E5a-I}(t)c^{p,i}_{E5a-I}(t)\cos\left(2\pi f_{L5}t\right) + Ac^{s,i}_{E5a-Q}(t)c^{p,i}_{E5a-Q}(t)\sin\left(2\pi f_{L5}t\right) \tag{2}$$

In this equation, A denotes the signal amplitude, with the minimum total power of the received Galileo E5a signal being −155.25 dBW for the data and pilot components combined (OS SIS ICD, 2023). The term d^i refers to the E5a navigation message, which is encoded with a convolutional FEC encoder with a ½ rate for satellite i. The original E5a navigation message has a data rate of 25 bps, and d^i has a final rate of 50 sps after encoding, resulting in a symbol duration of 20 ms. The sequences c^s_{E5a-I} and c^s_{E5a-Q} correspond to 20-bit and 100-bit secondary codes, respectively, encoded via the P/NRZ/L format. These codes are clocked at 1 kHz; thus, each bit lasts 1 ms. $c^{p,i}_{E5a-I}$ and $c^{p,i}_{E5a-Q}$ are the primary data and pilot component PRN codes, respectively, for satellite i. These primary codes, also in P/NRZ/L format, are 10,230 chips long and are clocked at 10.23 MHz, resulting in a code period of 1 ms.

The c^p_{E5a-I} and c^p_{E5a-Q} PRN codes are generated as a combination of two m-sequences, truncated to the appropriate length. The two m-sequences are generated by two parallel LFSRs of 14 cells, without any shift. The full Galileo E5a code generation is provided in OS SIS ICD (2023). The Galileo E5a code properties retrieved from Miret (2005) and Gao (2008), which do not consider Doppler residuals or blanking, are summarized in Table 2.

An additional set of assumptions regarding the signal definition is considered in this paper to assess the impact of blanking on the code properties. First, the navigation data d are always assumed to remain constant at unity during the integration time. Second, the secondary codes c^s_{L5I}, c^s_{L5Q}, $c^{s,i}_{E5a-I}$, and $c^{s,i}_{E5a-Q}$ are also assumed to be equal to unity during the integration time. An analysis of the secondary Neuman–Hofman codes (Neuman & Hofman, 1971) c^s_{L5I} and c^s_{L5Q} with respect to acquisition, bit synchronization, and narrowband interference protection has been reported by Zou et al. (2009), and an analysis of the secondary Galileo E5a codes $c^{s,i}_{E5a-I}$ and $c^{s,i}_{E5a-Q}$ with respect to acquisition has been reported by Shivaramaiah et al. (2008).

TABLE 2

c^p_{E5a-I} and c^p_{E5a-Q} Code Properties Without Considering Doppler Residuals or Blanker

Max. Auto-Correlation Sidelobe (dB)		Max. Cross-Correlation (dB)	
c^p_{E5a-I}	c^p_{E5a-Q}	c^p_{E5a-I}	c^p_{E5a-Q}
−28.9	−28.7	−26.0	−25.5

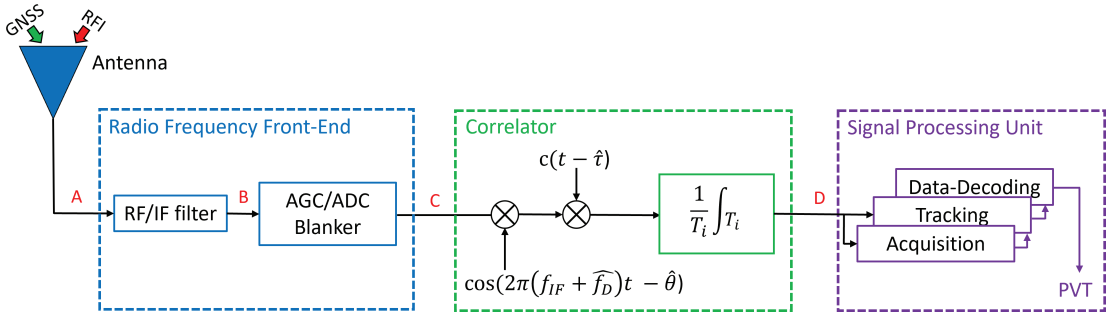

FIGURE 1 Generic airborne civil aviation GNSS receiver block scheme

3.2 | Generic Airborne GNSS DFMC Receiver Scheme

In this section, the structure of a generic airborne civil aviation GNSS receiver, along with the behavior and impact of its components, is introduced. Figure 1 presents the generic DFMC receiver structure.

The signal reception process begins at the antenna, which captures all of the in-band incoming signals, corresponding to a mixture of GNSS signals and undesirable RFI signals. The signals received at the antenna port, indicated as point A in Figure 1, are then passed to the RFFE block.

Multiple operations are performed in the RFFE block. First, the received signals are amplified, shifted from their original carrier frequency to a lower intermediate frequency, and filtered by the radio frequency/intermediate frequency (RF/IF) filter to obtain the signal at point B in Figure 1. The resulting signal is then digitized by an analog-to-digital converter (ADC) coupled with an automatic gain controller (AGC), which is responsible for minimizing the losses caused by quantization (Bastide et al., 2003). The temporal blanker is then introduced at this point (RTCA, 2004).

The temporal blanker is the countermeasure selected by civil aviation standards to mitigate the impact of pulsed RFI, such as DME/TACAN or JTIDS/MIDS signals. Note that the final implementation depends on the receiver manufacturer, as the exact structure of the temporal blanker is not standardized; three possible blanker implementations have been reported by Garcia-Pena et al. (2019; Garcia-Pena, Macabiau, Julien et al., 2020; Garcia-Pena, Macabiau, Novella et al., 2020). The temporal blanker is a device that blanks (sets to zero) the I/Q time samples of the incoming signal (mixture of signals) that have an instantaneous power envelope over a fixed threshold (RTCA, 2004). Figure 2(a) illustrates the instantaneous blanker application defined in RTCA (2004), where the blanking threshold is expressed in volts (V), and Figure 2(b) shows the normalized instantaneous power envelope along with durations.

At the RFFE block output, the digitized and blanked mix of GNSS and RFI signals at point C is fed to the correlator, which multiplies the signal by two local replicas (a sinusoid and an unblanked code) and coherently accumulates the resulting signal for T_i seconds, where T_i is the coherent integration time. At this stage, the simulations are processed, and the impact of the Doppler residuals and blanking is analyzed, as discussed in the following sections.

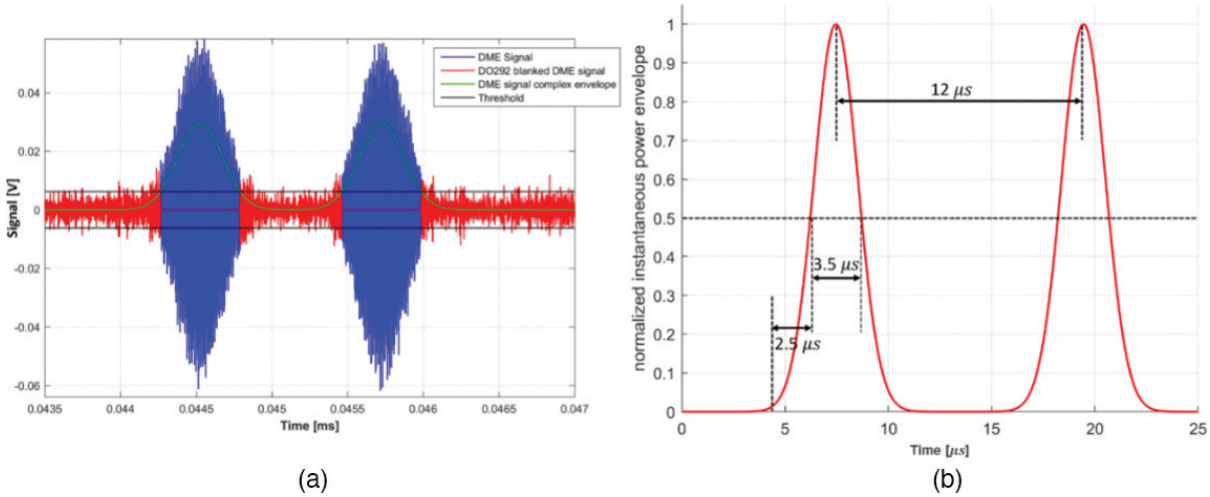

FIGURE 2 (a) Illustration of the RTCA DO-292 instantaneous blanker behavior over a DME signal; (b) normalized instantaneous power envelope of a DME/TACAN signal

Finally, at the output of the GNSS DFMC correlator (point D in Figure 1), the basic operations of the GNSS receiver, i.e., the acquisition, tracking, and demodulation of the GNSS signals, are performed, and the position, velocity, and time (PVT) are retrieved.

4 | SIMULATION METHODOLOGY

This section presents the simulation methodology used to evaluate the code correlation properties in the presence of a blanker. The goal of the simulation is to provide detailed statistics on these properties, focusing on the maximum values and quantiles (90%, 95%, 99%, 99.9%, 99.99%, and 99.999%) of the auto-correlation sidelobes and cross-correlation values. Additionally, the impact of Doppler residuals is assessed in the no-blanking scenario.

To ensure realistic conditions reflective of aviation applications, the simulation parameters were carefully selected. For instance, *bdc* values up to 75% were simulated to cover the worst-case scenario found in the RTCA DO-292, corresponding to a *bdc* of 63% near Harrisburg, PA, at FL400. The simulation settings are detailed as follows:

- The simulation included all 210 code pairs assigned in IS-GPS-705J (2022) for the GPS L5I/Q code family and the 50 code pairs assigned in OS SIS ICD (2023) for the Galileo E5a-I/Q code family.
- *bdc* values of 0%–75% were tested with a 15% step to comprehensively cover possible scenarios, including the RTCA worst-case scenario.
- For the 0% *bdc* scenario, Doppler residuals between –10 kHz and 10 kHz were evaluated, with a 50-Hz step.
- All possible code delays were tested with a 1-chip step.
- An integration time of 1 ms was used for each simulation.

The methodology for obtaining the quantiles and maximum values consists of four main steps:

1. Select *bdc* and the code pair.

2. Perform operations on the incoming code (application of blanking or Doppler residuals).
3. Apply a correlation operation with code replica.
4. Determine the maximum values and quantiles.

The four steps are detailed below.

1. Select *bdc* and the code pair: A *bdc* value is chosen from a range of 0%–75% with a 15% step, and a GPS L5 or Galileo E5a code pair $\left(c^{p,i}, c^{p,j}\right)$ is selected, where $i = j$ for auto-correlation and $i \neq j$ for cross-correlation. The indices i and j denote the incoming code and replica generated by the receiver, respectively.

2. Perform operations on the incoming code

2-a. Blanking (*bdc* higher than 0%)

2-a-1. Determine the number of chips/blocks to be blanked: The number of chips N_c to be blanked is determined as follows:

$$N_c = \lceil bdc \cdot 10230 \rceil \tag{3}$$

where $\lceil \cdot \rceil$ indicates rounding up to the nearest integer. Given that DME/TACAN RFI signals are the main contributor to *bdc* (RTCA, 2004), this paper assumes that blanked chips are grouped into blocks of 200 chips, hereafter referred to as blanked blocks. The length of each blanked block (200 chips) approximately corresponds to the duration of one DME/TACAN pulse pair (20 μs), as depicted in Figure 2(b).

The total number of blanked blocks required to obtain N_c blanked chips is calculated as follows:

$$N_b = \lceil N_c / 200 \rceil \tag{4}$$

It must be noted that one blanked block may contain fewer than 200 chips to reach exactly N_c.

2-a-2. Determine the starting indices of the blanked blocks: The starting indices of the N_b blanked blocks are randomly chosen, following a uniform distribution over the 10,230 chips while ensuring that the blocks do not overlap. This random process is repeated 100 times to ensure a sufficient number of different sets of the blanked block starting indices for extracting maximum values and selected quantiles.

2-b. Doppler residuals (0% *bdc* only)

Doppler residuals, i.e., sinusoids with frequencies equal to the offsets between the received signals and the local carrier replicas, ranging from –10 kHz to 10 kHz are applied to the incoming codes with a 50-Hz step.

3. Apply a correlation operation with code replica: For each set of blanked block starting indices, the incoming code $c^{p,i}$ is blanked. Figure 3 illustrates the blanking process for the incoming code, where two blocks of 200 chips are blanked in $c^{p,1}_{L5-I}$ for demonstration purposes.

The blanked or frequency-shifted code $c^{p,i}|_{N_b}$ is then multiplied by the non-blanked, non-shifted local replica $c^{p,j}$ in the frequency domain, which corresponds to the cross-ambiguity function (CAF) in the time domain, denoted as $S_{i,j}$. The calculation is performed in the frequency domain, as it directly provides results for all code delays with a step of one chip (Borre et al., 2007). The mathematical model of $S_{i,j}$ is given as follows:

$$S^n_{i,j} = \frac{\left|\mathrm{IFFT}\left(\mathrm{FFT}\left(c^{p,i}_{X-Y}|_{N_b}\right) \cdot \mathrm{FFT}^*\left(c^{p,j}_{X-Y}\right)\right)\right|}{10230} \tag{5}$$

where we have the following:

- FFT and IFFT represent the fast Fourier transform and inverse fast Fourier transform, respectively.
- FFT* denotes the complex conjugate of FFT.
- $c_{X-Y}^{p,i}$ and $c_{X-Y}^{p,j}$ are the i-th and j-th codes of code family X (GPS L5 or Galileo E5a) and channel Y (I or Q), respectively.
- $s(t)|_{N_b}$ is a signal $s(t)$ blanked for N_b blanked blocks.
- n denotes the n-th iteration with random sets of starting indices for blanked blocks.

4. Determine the maximum values and quantiles: For each *bdc* value, steps 1–3 are repeated to analyze all code pairs (i, j). For each pair, the CAF $S_{i,j}(f_D)$ is calculated across all 100 sets of blanked block starting indices. These values are stored in a large list, along with the $S_{i,j}$ values from all other code pairs. The entire list is then sorted in ascending order, allowing the selected quantiles and maximum values to be directly retrieved. Auto-correlation values are obtained via code pairs (i, i), whereas cross-correlation values are determined via code pairs $(i, j)_{i \neq j}$.

Steps 1–4 are repeated for each *bdc* setting to obtain the complete statistics on the GPS L5 and Galileo E5a code properties. Note that all derivations are conducted in the discrete domain, as the difference between discrete and continuous models with respect to the CAF is negligible (Foucras et al., 2017).

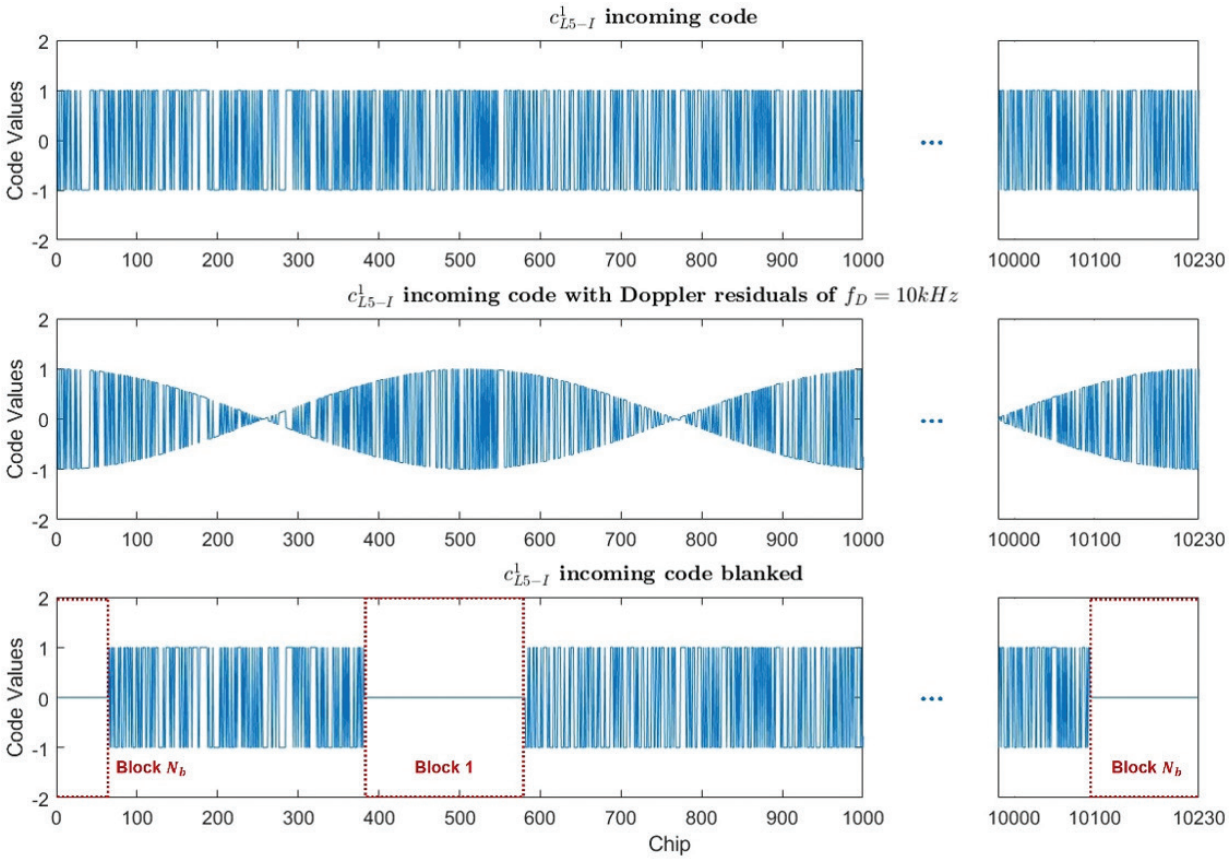

FIGURE 3 Application of Doppler residuals and blanking for GPS L5I PRN 1 code, $c_{L5-I}^{p,1}$, where 10-kHz Doppler residual is applied and two blocks of 200 chips are blanked

5 | RESULTS

This section presents the auto-correlation and cross-correlation properties of the GPS L5I/Q and Galileo E5a-I/Q codes. This section is divided into two main parts: the first subsection focuses on the auto-correlation main peaks and sidelobes, whereas the second section focuses on the cross-correlation values. In each subsection, we confirm that the classical results from the literature are retrieved when the effects of blanking and Doppler residuals are not considered. Then, the correlation properties are presented, accounting only for Doppler residuals, and finally, the impact of blanking for civil aviation applications is discussed.

5.1 | Auto-Correlation Results

In this subsection, the auto-correlation properties, specifically the main peaks and sidelobes, are investigated. If the auto-correlation main peaks are degraded, the minimal detection threshold used by the receiver must be lowered accordingly, while ensuring that the sidelobes are not mistakenly identified as the main peak. Otherwise, an incoming signal with a low carrier-to-noise density ratio (C/N_0) will not be detected. The auto-correlation main peaks of the GPS L5I/Q and Galileo E5a-I/Q code families in the presence of a blanker are provided in Table 3.

The auto-correlation main peak values in Table 3 indicate that GPS L5I/Q and Galileo E5a-I/Q lose the same amount of auto-correlation power, as the same percentage of samples is set to zero with the implementation of a blanker. The auto-correlation main peak values decrease significantly as *bdc* increases, falling to −8.0 dB in the RTCA DO-292 worst-case scenario (*bdc* ≈ 60%) and reaching −12.0 dB at 75% *bdc*.

Tables 4–7 present statistics for the auto-correlation sidelobes in the presence of blanking (from 0% to 75%) for GPS L5I and L5Q and Galileo E5a-I and E5a-Q, respectively. A quantile q indicates that q% of the autocorrelation sidelobes for a given *bdc* are below the value indicated in the table for any code pair $(c^{p,i}, c^{p,i})$, any code delays that are multitudes of 1 chip, and any random blanking block indices. For example, from the 95% quantile considering 30% *bdc* (line 2, column 4) of Table 4, it can be interpreted that 95% of the auto-correlation sidelobes for any pair $(c^{p,i}, c^{p,i})$ of GPS L5I codes are below −35.8 dB. It should be noted that the first column of each table (*bdc* = 0% with Doppler) is dedicated to the properties in the presence of Doppler residuals ranging from −10 kHz to 10 kHz without a blanker.

From the simulation results, four conclusions can be drawn:

1. From Tables 4–7, we observe that the maximum auto-correlation sidelobe values, without Doppler and blanking effects, are nearly identical to those reported in the literature, varying by up to 0.4 dB, except for GPS L5I, which

TABLE 3
GPS L5I/Q and Galileo E5a-I/Q Auto-Correlation Main Peak Results in the Presence of a Blanker

Auto-correlation main peak (dB)						
bdc	0%	15%	30%	45%	60%	75%
$c^p_{L5I}, c^p_{L5Q}, c^p_{E5a-I}, c^p_{E5a-Q}$	0.0	−1.4	−3.1	−5.2	−8.0	−12.0

TABLE 4
GPS L5I Auto-Correlation Sidelobe (dB) Results in the Presence of a Blanker

bdc / quantiles	0% with Doppler	0%	15%	30%	45%	60%	75%
90%	−36.5	−35.8	−36.5	−37.3	−38.3	−39.7	−41.8
95%	−35.3	−34.4	−35.0	−35.8	−36.9	−38.3	−40.3
99%	−33.4	−32.2	−32.9	−33.6	−34.6	−35.9	−38.0
99.9%	−31.7	−30.4	−30.9	−31.6	−32.5	−33.8	−35.8
99.99%	−30.4	−29.2	−29.6	−30.3	−31.2	−32.4	−34.4
99.999%	−29.4	−28.7	−28.8	−29.3	−30.1	−31.4	−33.3
Maximum	−27.7	−28.2	−26.7	−26.7	−27.2	−28.2	−30.3

TABLE 5
GPS L5Q Auto-Correlation Sidelobe (dB) Results in the Presence of a Blanker

bdc / quantiles	0% with Doppler	0%	15%	30%	45%	60%	75%
90%	−36.5	−35.8	−36.5	−37.3	−38.3	−39.7	−41.8
95%	−35.3	−34.4	−35.0	−35.8	−36.9	−38.2	−40.3
99%	−33.4	−32.2	−32.9	−33.6	−34.6	−35.9	−38.0
99.9%	−31.6	−30.3	−30.9	−31.6	−32.5	−33.8	−35.8
99.99%	−30.4	−29.0	−29.6	−30.2	−31.1	−32.4	−34.4
99.999%	−29.4	−28.6	−28.7	−29.2	−30.1	−31.4	−33.3
Maximum	−27.5	−28.6	−26.7	−27.0	−27.8	−28.2	−30.3

TABLE 6
Galileo E5a-I Auto-Correlation Sidelobe (dB) Results in the Presence of a Blanker

bdc / quantiles	0% with Doppler	0%	15%	30%	45%	60%	75%
90%	−36.5	−35.8	−36.5	−37.3	−38.5	−39.9	−41.8
95%	−35.3	−34.3	−34.9	−35.8	−36.9	−38.3	−40.3
99%	−33.4	−31.8	−32.6	−33.5	−34.5	−35.9	−38.0
99.9%	−31.6	−30.0	−30.6	−31.4	−32.4	−33.8	−35.7
99.99%	−30.4	−29.0	−29.4	−30.1	−31.0	−32.3	−34.3
99.999%	−29.4	−28.6	−28.6	−29.1	−30.0	−31.3	−33.2
Maximum	−27.5	−28.6	−26.7	−27.0	−27.7	−28.6	−30.7

shows a 1-dB difference. This discrepancy can be attributed to the different number of codes analyzed in our simulations compared with previous studies. Figure 4 presents the maximum auto-correlation sidelobe for each PRN, with PRN 164 exhibiting the highest value of −28.2 dB. When only the first 37 GPS L5I codes are assessed, as shown in Figure 4, the maximum auto-correlation sidelobe is −29.2 dB, which matches the value reported in the literature, as indicated in Table 1.

2. In the first columns of Tables 4–7 (*bdc* = 0% with Doppler), which consider the impact of Doppler residuals ([−10, 10] kHz), the effect on the auto-correlation sidelobes is minor: the maximum sidelobes increase by up to 1.1 dB for GPS

TABLE 7
Galileo E5a-Q Auto-Correlation Sidelobe (dB) Results in the Presence of a Blanker

bdc / quantiles	0% with Doppler	0%	15%	30%	45%	60%	75%
90%	−36.5	−35.8	−36.5	−37.3	−38.5	−39.9	−41.8
95%	−35.3	−34.3	−34.9	−35.8	−36.9	−38.3	−40.3
99%	−33.4	−31.8	−32.6	−33.5	−34.5	−35.9	−38.0
99.9%	−31.6	−29.9	−30.6	−31.3	−32.4	−33.8	−35.7
99.99%	−30.3	−29.1	−29.4	−30.1	−31.0	−32.3	−34.3
99.999%	−29.3	−28.7	−28.6	−29.1	−30.0	−31.3	−33.3
Maximum	−27.7	−28.6	−26.8	−27.2	−27.5	−28.5	−30.9

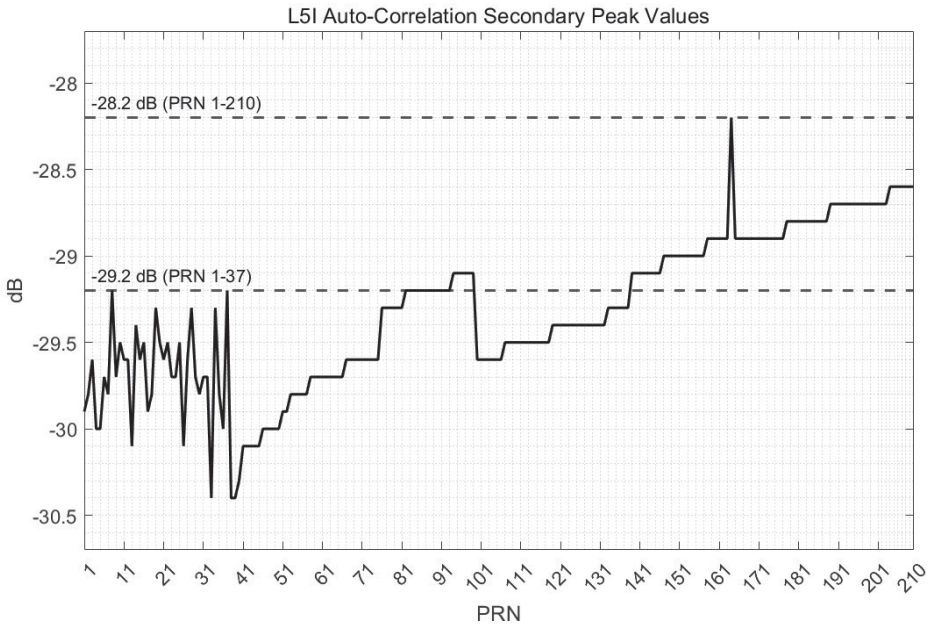

FIGURE 4 Maximum auto-correlation sidelobes for PRN codes
The maximum auto-correlation sidelobe was observed to be −29.2 dB for PRNs 1–37, consistent with the value reported in the literature; meanwhile, the maximum value increases to −28.2 dB when the entire set of 210 PRN codes is examined.

L5Q and Galileo E5a-I (Tables 5 and 6) and by 0.5 dB and 0.8 dB for GPS L5I and Galileo E5a-Q code families, respectively (Tables 4 and 7). This increase is significantly smaller than that observed for the GPS L1 C/A code family, where the increase can reach up to 4.8 dB (Foucras et al., 2017) owing to the greater code length (10,230 chips) and higher chipping rate (10.23 Mcps) of L5/E5a codes. The 4.8-dB increase for L1 C/A was also confirmed by the MATLAB simulations used in this work, by merely changing the analyzed codes from L5/E5a to L1 C/A.

3. In Tables 4–7, the auto-correlation sidelobes at each quantile, except for the maximum values, generally decrease as *bdc* increases. For example, in the worst-case scenario defined in the RTCA DO-292 (*bdc* ≈ 60%), the 90% quantiles of auto-correlation sidelobes are suppressed by approximately 4 dB for all of the L5/E5a code families. In contrast, the maximum sidelobes experience the greatest increases at a *bdc* of 15%, increasing by 1.5 dB to

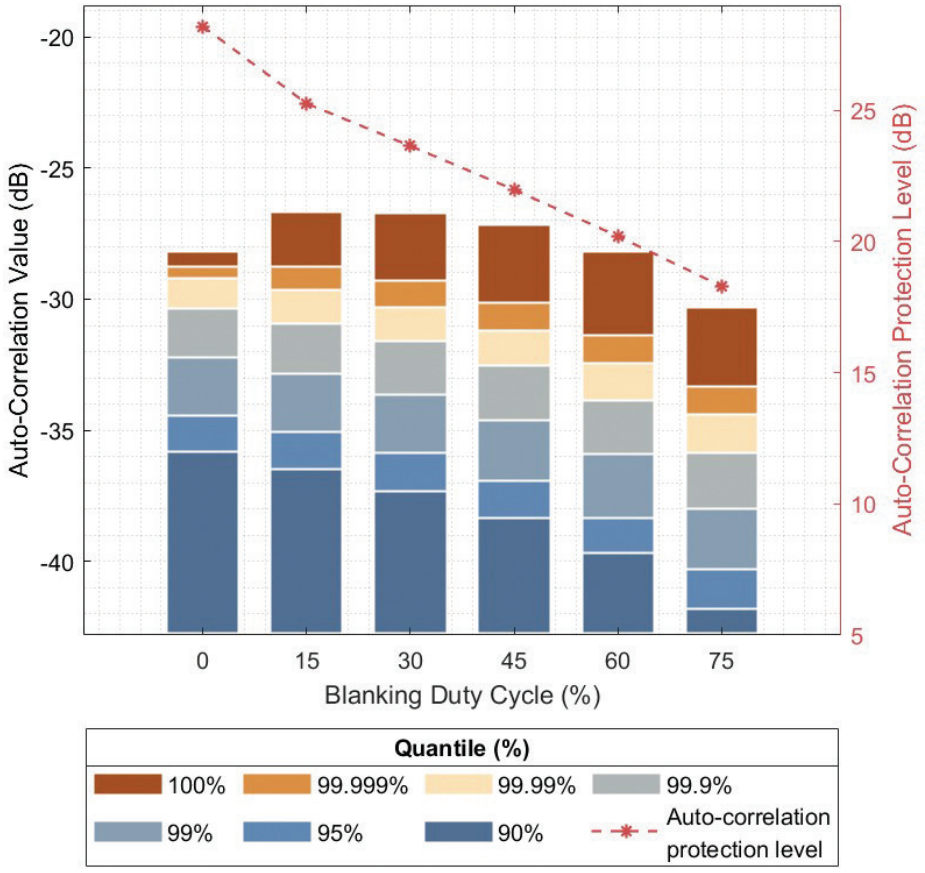

FIGURE 5 GPS L5I auto-correlation sidelobe statistics (dB) for selected quantiles in the presence of a blanker
The dashed line represents the auto-correlation protection level.

1.9 dB. As *bdc* exceeds 15%, the maximum sidelobes begin to steadily decrease, becoming nearly equal to the 0% *bdc* case at 60% *bdc*. Further increasing the *bdc* to 75% results in the maximum sidelobes being reduced by approximately 2 dB compared with the 0% *bdc* case.

4. Auto-correlation protection, defined as the margin between the auto-correlation main peak and the maximum sidelobe, consistently decreases as *bdc* increases, as shown in Figure 5. This decline is mainly due to the significant reduction in the main peak, which can decrease by up to 12 dB at a *bdc* of 75%, compared with increases in the maximum sidelobes, or a relatively small decrease at a *bdc* of 75%. As a result, protection levels fall from 28.6 dB (28.2 dB for L5I) at a *bdc* of 0% to 20.2–20.6dB at a *bdc* of 60%, decreasing further to 18.3–18.9 dB at a *bdc* of 75%, thereby increasing the risk of acquiring the sidelobe instead of the main peak. Despite this reduction, L5/E5a code families demonstrate better or equivalent auto-correlation protection levels up to a *bdc* of 60% compared with L1 C/A codes, which have a maximum auto-correlation sidelobe of approximately −19.2 dB in the presence of Doppler residuals (Foucras et al., 2017). Although Doppler residuals were not considered, L5/E5a codes with 60% *bdc* still maintain superior or comparable protection levels compared with L1 C/A codes, even in the presence of Doppler residuals, owing to the minimal impact of Doppler residuals on L5/E5a codes.

5.2 | Cross-Correlation Results

In this subsection, the cross-correlation code properties obtained from our simulation results are introduced and compared with the results obtained for auto-correlation properties. Cross-correlation properties are crucial for ensuring that weak signals are not masked by the noise generated by cross-correlation with stronger signals during the acquisition stage (Qaisar & Dempster, 2007).

Tables 8–11 present simulation results for selected quantiles of cross-correlation values in the presence of blanking (from 0% to 75%) for GPS L5I and L5Q and

TABLE 8
GPS L5I Cross-Correlation (dB) Results in the Presence of a Blanker

bdc / quantiles	0% with Doppler	0%	15%	30%	45%	60%	75%
90%	−36.5	−35.8	−36.5	−37.3	−38.3	−39.7	−41.8
95%	−35.3	−34.4	−35.0	−35.8	−36.9	−38.2	−40.3
99%	−33.4	−32.2	−32.9	−33.6	−34.5	−35.9	−38.0
99.9%	−31.7	−30.3	−30.9	−31.6	−32.5	−33.8	−35.8
99.99%	−30.4	−28.8	−29.4	−30.2	−31.1	−32.4	−34.4
99.999%	−29.3	−27.8	−28.4	−29.1	−30.0	−31.3	−33.3
Maximum	−26.4	−26.4	−25.4	−25.4	−26.6	−27.2	−29.9

TABLE 9
GPS L5Q Cross-Correlation (dB) Results in the Presence of a Blanker

bdc / quantiles	0% with Doppler	0%	15%	30%	45%	60%	75%
90%	−36.5	−35.8	−36.5	−37.3	−38.3	−39.7	−41.8
95%	−35.3	−34.4	−35.0	−35.8	−36.9	−38.2	−40.3
99%	−33.4	−32.2	−32.9	−33.6	−34.5	−35.9	−38.0
99.9%	−31.7	−30.3	−30.9	−31.6	−32.5	−33.8	−35.8
99.99%	−30.4	−28.8	−29.4	−30.2	−31.1	−32.4	−34.4
99.999%	−29.3	−27.8	−28.4	−29.1	−30.0	−31.3	−33.3
Maximum	−26.3	−26.4	−25.2	−25.8	−26.6	−27.1	−29.7

TABLE 10
Galileo E5a-I Cross-Correlation (dB) Results in the Presence of a Blanker

bdc / quantiles	0% with Doppler	0%	15%	30%	45%	60%	75%
90%	−36.5	−35.7	−36.4	−37.3	−38.3	−39.7	−41.8
95%	−35.3	−34.1	−34.9	−35.7	−36.8	−38.2	−40.3
99%	−33.4	−31.7	−32.4	−33.3	−34.4	−35.8	−37.9
99.9%	−31.6	−29.7	−30.3	−31.2	−32.2	−33.7	−35.7
99.99%	−30.2	−28.3	−29.0	−29.8	−30.8	−32.2	−34.3
99.999%	−29.0	−27.2	−27.9	−28.7	−29.7	−31.1	−33.2
Maximum	−25.7	−25.7	−25.0	−25.8	−26.1	−28.1	−29.4

TABLE 11
Galileo E5a-Q Cross-Correlation (dB) Results in the Presence of a Blanker

bdc / quantiles	0% with Doppler	0%	15%	30%	45%	60%	75%
90%	−36.5	−35.7	−36.4	−37.3	−38.3	−39.7	−41.8
95%	−35.3	−34.1	−34.9	−35.7	−36.8	−38.2	−40.3
99%	−33.4	−31.7	−32.4	−33.3	−34.4	−35.8	−37.9
99.9%	−31.6	−29.7	−30.4	−31.2	−32.2	−33.7	−35.7
99.99%	−30.2	−28.3	−29.0	−29.8	−30.8	−32.2	−34.3
99.999%	−29.0	−27.2	−27.9	−28.7	−29.8	−31.1	−33.2
Maximum	−26.2	−26.2	−24.9	−25.5	−26.3	−27.8	−30.1

Galileo E5a-I and E5a-Q, respectively. As in Section 5.1, the first column presents results for Doppler residuals ([−10, 10] kHz) only. The second column of each table is dedicated to the properties observed without blanking, allowing for a comparison with results found in the literature.

The following conclusions can be drawn from the simulations results:

1. From Tables 8–11, we retrieved cross-correlation peaks for L5/E5a codes that closely match those reported in the literature, with differences of up to 0.7 dB in the absence of Doppler and blanker effects. This variance is also due to the different number of codes analyzed in our simulations compared with previous studies, as discussed in Section 5.1.
2. In the first columns (*bdc* = 0%) of Tables 8–11, where only Doppler residuals are considered, it is shown that Doppler residuals in the range of [−10, 10] kHz have a negligible effect on the maximum cross-correlation values, causing an increase of less than 0.1 dB. This behavior contrasts with the GPS L1 C/A case, where the same range of Doppler residuals can cause the cross-correlation peak to increase by as much as 4.9 dB (Foucras et al., 2017).
3. In Tables 8–11, although the blanking process with a 15% *bdc* increases the maximum cross-correlation values by up to 1.3 dB, further increases in *bdc* beyond 15% result in a consistent decrease in cross-correlation peaks across all quantiles. In the RTCA DO-292 worst-case scenario (*bdc* ≈ 60%), the maximum cross-correlations decrease by up to 2.4 dB compared with the 0% *bdc* case for E5a-I codes.
4. The dashed line in Figure 6 shows that higher *bdc* levels lead to lower cross-correlation protection, defined as the margin between the auto-correlation peak and the maximum cross-correlation values. This reduction occurs because the cross-correlation peaks experience relatively small changes compared with the significant reduction in the main auto-correlation peak, which can decrease by up to 8 dB in the RTCA DO-292 worst-case scenario. Cross-correlation protection levels decrease from approximately 26 dB at 0% *bdc* to slightly above the L1 C/A cross-correlation protection level of 19.1 dB (Foucras et al., 2017) around the RTCA DO-292 worst-case scenario. The protection levels further decrease to just above 17 dB at a *bdc* of 75%. This decline in cross-correlation protection increases the risk of mistakenly acquiring the cross-correlation peak instead of the auto-correlation main peak.

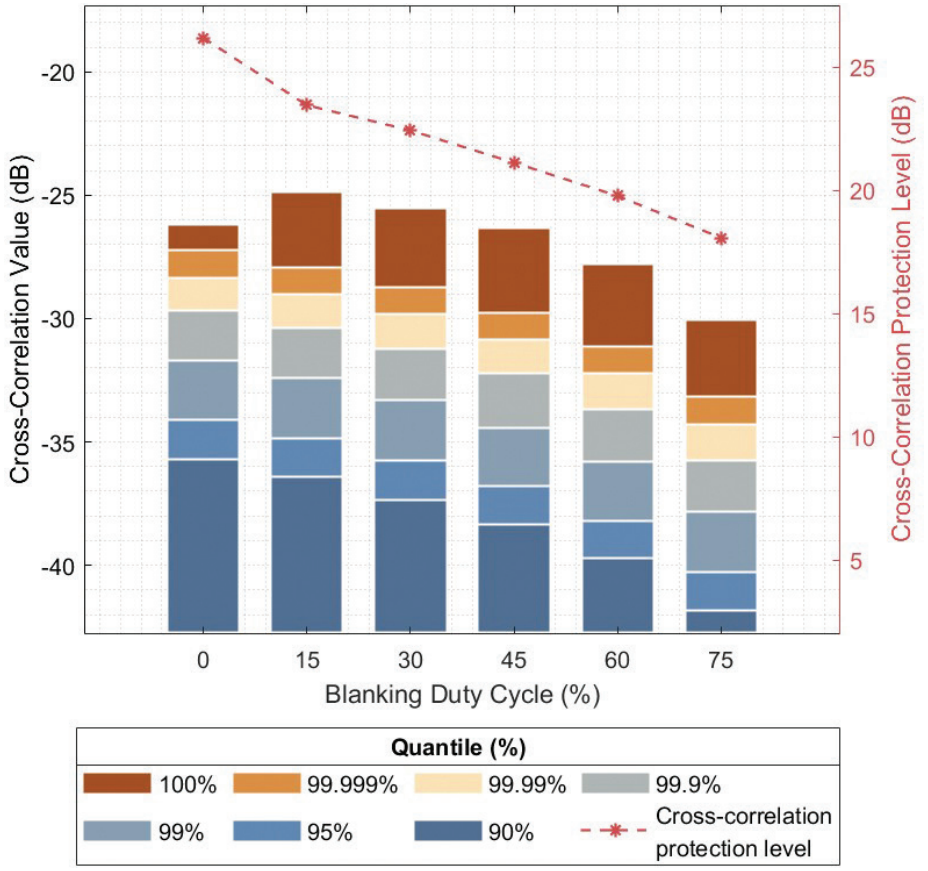

FIGURE 6 Galileo E5a-Q cross-correlation (dB) for selected quantiles in the presence of a blanker
The dashed line represents the correlation protection levels against cross-correlations.

6 | CONCLUSION

In this work, extensive simulations were performed to provide a statistical description of the auto-correlation and cross-correlation properties for the GPS L5I/Q and Galileo E5a-I/Q code families. First, the simulation results were found to be almost identical to the classical results for auto-correlation and cross-correlation found in the literature for GPS L5I/Q and Galileo E5a-I/Q, excluding the effects of Doppler residuals and blanking. The minor differences observed can be attributed to the different sets of codes used in this study compared with the literature. Second, statistics on the auto- and cross-correlation properties were provided while considering Doppler residuals only, within a classical range of [–10, 10] kHz. The findings indicate that Doppler residuals have a minimal impact on the correlation properties, owing to the greater code length and higher chipping rate of L5/E5a codes compared with those of L1 C/A. Notably, in the presence of Doppler residuals, the cross-correlation peaks remained the same, except for GPS L5Q, which exhibited a slight increase of less than 0.1 dB. These results are significantly better than those of the legacy GPS L1 C/A code family, where the increase in the maximum auto-correlation sidelobe and cross-correlation due to Doppler frequency in the same range can reach approximately 4.9 dB for an integration time of 1 ms (Foucras et al., 2017). Finally, this statistical description of the auto-correlation and cross-correlation properties was completed with the introduction of the blanker for the civil aviation context, where the *bdc* in the RTCA DO-292 worst-case scenario

can reach 63% (RTCA, 2004). For *bdc* values ranging from 0% to 75%, the most significant impact of the blanker was observed for the auto-correlation main peak, which can decrease by almost 8 dB in the worst-case scenario (*bdc* ≈ 60%). In contrast, the maximum auto-correlation sidelobes increase by less than 1.9 dB, and the cross-correlation peaks increase by less than 1.3 dB for both L5 and E5a, resulting in a reduction in protection against auto-correlation sidelobes and cross-correlations to 20.2–20.6 dB and 19.1–20.1 dB, respectively, in the worst-case scenario and to 18.3–18.9 dB and 17.4–18.1 dB at a *bdc* of 75%. In this scenario, a possible solution could be to lower the acquisition threshold to ensure that even the weakest signal is acquired in the presence of Doppler residuals and blanker. The simulations further demonstrated that although the correlation protection levels of L5/E5a codes decrease as *bdc* increases, they remain superior or comparable to the protection levels of the L1 C/A code family without blanking, even in the RTCA DO-292 worst-case scenario. However, further increases in *bdc* due to the rising trend in air traffic volume may diminish the correlation advantages that L5/E5a codes hold over L1 C/A codes. A study of the potentially positive effects of longer integration times on GNSS L5/E5a code properties in the presence of a blanker, as specified in civil aviation standards, is left for future work.

ACKNOWLEDGMENTS

This work was supported by the National Research Foundation of Korea funded by the Ministry of Science and ICT under Grant 2022M1A3C2069728, Future Space Education Center.

REFERENCES

Airbus. (2024). *Global market forecast 2024*. https://www.airbus.com/sites/g/files/jlcbta136/files/2024-07/GMF%202024-2043%20Presentation_4DTS.pdf

Bastide, F., Akos, D., Macabiau, C., & Roturier, B. (2003). Automatic gain control (AGC) as an interference assessment tool. *Proc. of the 16th International Technical Meeting of the Satellite Division of the Institute of Navigation (ION GPS/GNSS 2003),* Portland, OR, 2042–2053. https://www.ion.org/publications/abstract.cfm?articleID=5389

Betz, J. W., Cahn, C. R., Dafesh, P. A., Hegarty, C. J., Hudnut, K. W., Jones, A. J., Keegan, R., Kovach, K., Lenahan, L. S., Ma, H. H., Rushanan, J. J., Stansell, T. A., Wang, C. C., & Yi, S. K. (2006). L1C signal design options. *Proc. of the 2006 National Technical Meeting of the Institute of Navigation,* Monterey, CA, 685–697. https://www.ion.org/publications/abstract.cfm?articleID=6573

Borre, K., Akos, D. M., Bertelsen, N., Rinder, P., & Jensen, S. (2007). *A software-defined GPS and Galileo receiver: a single-frequency approach*. Birkhäuser. https://www.ocf.berkeley.edu/~marsy/resources/gnss/A%20Software-Defined%20GPS%20and%20Galileo%20Receiver.pdf

European Space Agency. (1999). *The European Space Agency and the European Commission sign contracts for the Galileo programme* [Press release]. https://www.esa.int/Newsroom/Press_Releases/The_European_Space_Agency_and_the_European_Commission_sign_contracts_for_the_Galileo_programme

Falcone, M., Hahn, J., & Burger, T. (2017). Galileo. In P. J. G. Teunissen & O. Montenbruck (Eds.), *Springer handbook of global navigation satellite systems* (pp. 242–272). Springer. https://doi.org/10.1007/978-3-319-42928-1_9

Foucras, M., Leclère, J., Botteron, C., Julien, O., Macabiau, C., Farine, P.-A., & Ekambi, B. (2017). Study on the cross-correlation of GNSS signals and typical approximations. *GPS Solutions*, *21*(2), 293–306. https://doi.org/10.1007/s10291-016-0556-7

Gao, G. X. (2008). *Towards navigation based on 120 satellites: Analyzing the new signals (Publication No. 3332824)* [Doctoral dissertation, Standford University]. ProQuest Dissertations and Theses Global.

Gao, G. X., & Enge, P. (2012). How many GNSS satellites are too many? *IEEE Transactions on Aerospace and Electronic Systems*, *48*(4), 2865–2874. https://doi.org/10.1109/TAES.2012.6324666

Garcia-Pena, A., Julien, O., Gakne, P. V., Macabiau, C., Mabilleau, M., & Durel, P. (2019). Efficient DME/TACAN blanking method for GNSS-based navigation in civil aviation. *Proc. of the 32nd International Technical Meeting of the Satellite Division of the Institute of Navigation (ION GNSS+ 2019),* Miami, FL, 1438–1452. https://doi.org/10.33012/2019.16993

Garcia-Pena, A., Macabiau, C., Julien, O., Mabilleau, M., & Durel, P. (2020). IGNSS computation models and values for GPS and GALILEO L5/E5a civil aviation receivers. *Proc. of the 33rd International Technical Meeting of the Satellite Division of the Institute of Navigation (ION GNSS+ 2020)*. https://doi.org/10.33012/2020.17571

Garcia-Pena, A., Macabiau, C., Novella, G., Julien, O., Mabilleau, M., & Durel, P. (2020). In-band RFI GNSS L5/E5a mask definition. *Proc. of the 33rd International Technical Meeting of the Satellite Division of the Institute of Navigation (ION GNSS+ 2020),* 188–205. https://doi.org/10.33012/2020.17540

Gold, R. (1967). Optimal binary sequences for spread spectrum multiplexing (corresp.). *IEEE Transactions on Information Theory*, *13*(4), 619–621. https://doi.org/10.1109/TIT.1967.1054048

Grabowski, J., & Hegarty, C. (2002). Characterization of L5 receiver performance using digital pulse blanking. *Proc. of the 15th International Technical Meeting of the Satellite Division of the Institute of Navigation (ION GPS 2002),* Portland, OR, 1630–1635. https://www.ion.org/publications/abstract.cfm?articleID=2176

Hegarty, C., Van Dierendonck, A. J., Bobyn, D., Tran, M., & Grabowski, J. (2000). Suppression of pulsed interference through blanking. *Proc. of the IAIN World Congress and the 56th Annual Meeting of the Institute of Navigation (2000),* San Diego, CA, 399–408. https://www.ion.org/publications/abstract.cfm?articleID=792

IS-GPS-705J: Navstar GPS space segment/user segment L5 interfaces. (2022).

Kaplan, E. D., & Hegarty, C. (2005). *Understanding GPS: Principles and applications* (2nd ed.). Artech House Publishers. https://ieeexplore.ieee.org/document/9106073

Macabiau, C., Calmettes, V., Vigneau, W., Ries, L., & Issler, J.-L. (2002). L5 code properties. *GNSS 2002*. Copenhagen.

Miret, E. A. (2005). *Galileo code properties*. European Space Memorandum, ESA-DEUI-NGMEMO/01798.

Morton, Y. T. J., Tsui, J. B. Y., Lin, D. M., Liou, L. L., Miller, M. M., Zhou, Q., French, M. P., & Schamus, J. (2003). Assessment and handling of CA code self-interference during weak GPS signal acquisition. *Proc. of the 16th International Technical Meeting of the Satellite Division of the Institute of Navigation (ION GPS/GNSS 2003),* Portland, OR, 646–653. https://www.ion.org/publications/abstract.cfm?articleID=5238

Neuman, F., & Hofman, L. (1971). New pulse sequences with desirable correlation properties. In *Proceedings of the IEEE National Telemetry Conference,* 272–282.

Novella, G., Pena, A. J. G., Macabiau, C., Martineau, A., Ladoux, P., Estival, P., & Troubet-Lacoste, O. (2022). GNSS acquisition thresholds for civil aviation GNSS receivers. *Proc. of the 35th International Technical Meeting of the Satellite Division of the Institute of Navigation (ION GNSS+ 2022)*, Denver, CO, 166–191. https://doi.org/10.33012/2022.18357

OS SIS ICD: GALILEO open service signal-in-space interface control document. (2023).

Qaisar, S., & Dempster, A. (2007). An analysis of L1-C/A cross correlation and acquisition effort in weak signal environments. In *Proceedings of IGNSS2007*. https://doi.org/10.26190/unsworks/717

Qaisar, S. U., & Dempster, A. G. (2011). Cross-correlation performance assessment of Global Positioning System (GPS) L1 and L2 civil codes for signal acquisition. *IET Radar, Sonar & Navigation*, *5*(3), 195–203. https://doi.org/10.1049/iet-rsn.2009.0207

Rebeyrol, E. (2007). *Galileo signals and payload optimization* [Doctoral dissertation, Telecom ParisTech, Paris, France]. https://pastel.hal.science/pastel-00004315/file/These_Rebeyrol_V2.pdf

RTCA. (2004). *DO 292: Assessment of radio frequency interference relevant to the GNSS L5/E5A frequency band*. Washington, DC: RTCA. https://my.rtca.org/productdetails?id=a1B36000001IchPEAS

Shivaramaiah, N. C., Dempster, A. G., & Rizos, C. (2008). Exploiting the secondary codes to improve signal acquisition performance in Galileo receivers. *Proc. of the 21st International Technical Meeting of the Satellite Division of the Institute of Navigation (ION GNSS 2008),* Savannah, GA, 1497–1506. https://www.ion.org/publications/abstract.cfm?articleID=8063

Soualle, F. (2009). Correlation and randomness properties of the spreading coding families for the current and future GNSSs. In *Fourth European Workshop on GNSS Signals and Signal Processing, Oberpfaffenhofen, Germany*.

Soualle, F., Soellner, M., Wallner, S., Avila-Rodriguez, J.- A., Hein, G. W., Barnes, B., Pratt, T., Ries, L., Winkel, J., Lemenager, C., & Erhard, P. (2005). Spreading code selection criteria for the future GNSS Galileo. *Proc. of the European Navigation Conference GNSS*, 19–22.

Spilker, J. J., Jr. (1996). GPS signal structure and theoretical performance. In B. Parkinson, J. J. Spilker Jr., P. Axelrad, & P. Enge (Eds.), *Global Positioning System: Theory and applications*, 57–119. American Institute of Aeronautics and Astronautics. https://doi.org/10.2514/5.9781600866388.0057.0119

Spilker, J. J., Jr., & Van Dierendonck, A. J. (2001). Proposed new L5 civil GPS codes. *NAVIGATION*, *48*(3), 135–143. https://doi.org/10.1002/j.2161-4296.2001.tb00237.x

Tawk, Y., Botteron, C., Jovanovic, A., & Farine, P. A. (2012). Analysis of Galileo E5 and E5ab code tracking. *GPS Solutions*, *16*, 243–258. https://doi.org/10.1007/s10291-011-0226-8

Tran, M. (2004). Performance evaluations of the new GPS L5 and L2 Civil (L2C) signals. *NAVIGATION*, *51*(3), 199–212. https://doi.org/10.1002/j.2161-4296.2004.tb00351.x

Van Diggelen, F. (2009). *A-GPS: Assisted GPS, GNSS, and SBAS*. Artech House. https://ieeexplore.ieee.org/document/9100796

Wallner, S., Avila-Rodriguez, J. A., Hein, G. W., & Rushanan, J. J. (2007). Galileo E1 OS and GPS L1C pseudo random noise codes-requirements, generation, optimization and comparison. *Proc. of the 20th International Technical Meeting of the Satellite Division of the Institute of Navigation (ION GNSS 2007),* Fort Worth, TX, 1549–1563. https://www.ion.org/publications/abstract.cfm?articleID=7359

Zeta Associates. (2019). *High L5 blanking at HNL WRS HNL TACAN study* [Presentation]. RTCA SC-159 WG-6.

Zeta Associates. (2021). *High L5 blanking at ZLA WRS, update to HNL TACAN study* [Presentation]. RTCA SC-159 WG-6.

Zou, D., Deng, Z., Huang, J., Liu, H., & Yang, L. (2009). A study of Neuman Hoffman codes for GNSS application. *Proc. of the 5th International Conference on Wireless Communications, Networking and Mobile Computing,* Beijing, China, 1–4. https://doi.org/10.1109/WICOM.2009.5305353

How to cite this article: Kim, S., Gault, N., Jo, Y., Yoon, H., Park, B., Garcia-Pena, A., Macabiau, C., & Akos, D. M. (2025). GNSS L5/E5a code properties in the presence of a blanker. *NAVIGATION, 72*(2). https://doi.org/10.33012/navi.700